Opportunistic Error Correction for MIMO-OFDM: From Theory to Practice

Xiaoying Shao and Cornelis H. Slump
University of Twente, Enschede, 7500AE, The Netherlands
Email: x.shao@utwente.nl, c.h.slump@utwente.nl

Abstract—Opportunistic error correction based on fountain codes is especially designed for the MIMO-OFDM system. The key point of this new method is the tradeoff between the code rate of error correcting codes and the number of sub-carriers in the channel vector to be discarded. By transmitting one fountain-encoded packet over a single sub-carrier per antenna, the ADC is allowed to only take care of the sub-carriers with high energy in the channel vector. In such a case, the power in the ADC is reduced by quantizing the received signal coarsely. Correspondingly, this approach can afford higher level of noise floor than the joint coding scheme adopted by the current MIMO-OFDM system. In this paper, we evaluate its performance in the aspect of mitigating the noise and interference. At the same code rate, simulation results show that opportunistic error correction works better (i.e. requires lower SNR) than the FEC layers defined in the IEEE 802.11n standard. With respect to RCPC with interleaving, the SNR gained by opportunistic error correction decreases as the multiplexing gain increases. Furthermore, we evaluate their performance in the real world. This novel approach does not have the same SNR gain in practice as in the simulation, compared to the FEC layers in the IEEE 802.11n standard. Measurement results show that this new scheme survives in most of the channel conditions (i.e. 92%) with respect to RCPC with interleaving (i.e. 86%) and the LDPC code from the IEEE 802.11n standard (i.e. around 80%).

Index Terms—opportunistic error correction, MIMO, OFDM, ADC, FEC, RCPC, LDPC

I. Introduction

Multiple-Input Multiple-Output (MIMO) technology has attracted a lot of attention in wireless communications, due to its high data rate without additional band-width or transmission power [1]-[4]. Combining Orthogonal Frequency Division Multiplexing (OFDM) with MIMO enables a relative easy implementation of wireless MIMO systems [5]-[6]. The OFDM signal is the superposition of low rate streams modulated at different frequencies, resulting in its time-domain dynamic range increasing with the number of sub-carriers [7]. The high Peak-to-Average Power Ratio (PAPR) requires high-resolution Digital-to-Analog Converters (DACs) at the transmitter and Analog-to-Digital Converters (ADCs) at the receiver. For MIMO systems, the received signal at each antenna is the superposition of the OFDM signals from all transmitting antennas [1]. Correspondingly, the received OFDM signal at a MIMO system has even higher PAPR compared to the Single-Input-Single-Output (SISO) system. The ADC can consume 50% of the total amount of baseband power [8], and its power consumption is exponentially proportional to its resolution [9]. Most of wireless receivers are battery-powered and cannot afford high power consumption. Reducing the resolution of ADCs is equivalent to raise the quantization noise (i.e. Bit Error Rate (BER)). Therefore, we propose a cross coding scheme in order to use low-resolution ADCs at wireless receivers without compromising the communication quality.

To achieve reliable communication at a high data rate, error correction codes have to be employed in MIMO-OFDM systems [10]-[12]. Over a finite block length, coding jointly over all the sub-carriers yields a smaller error probability that can be achieved by coding separately over the sub-carriers at the same rate [1]. This theory has been applied in practical SISO-OFDM and MIMO-OFDM systems, such as WLAN and DVB systems [14]-[17]. In MIMO-OFDM systems like the IEEE 802.11n system [14], source data is encoded across all the transmit antennas and the entire transmission band. For a $M \times M$ MIMO-OFDM system, the joint coding scheme utilizes the fact that sub-carriers with high-energy can compensate for those with low-energy over the M parallel channels, but its drawback is that each sub-carrier must be decoded. With the joint coding scheme [1], the maximum level of the noise floor (NF) is limited to the dynamic range of the M parallel channels. That shows the resolution of ADCs is proportional to the dynamic range of the channel vector.

In this paper, we propose an energy-efficient error correction scheme based on fountain codes to reduce the power consumption in ADCs for MIMO-OFDM systems. Fountain codes can reconstruct the source file by collecting enough packets. It does not matter which packet is received. We only need to receive a certain number of packets. Therefore, we propose to transmit a fountain-encoded packet over a sub-carrier per antenna.

Manuscript received July 16, 2013; revised September 23, 2013.
This work was supported by the Dutch Ministry of Economic Affairs under the IOP Generic Communication-Senter Novem Program.
Corresponding author email: x.shao@utwente.nl.
doi:10.12720/jcm.8.9.540-549

Multiple packets are transmitted simultaneously, using frequency division multiplexing and space division multiplexing. Because of fountain codes, the receiver does not have to take care of all the parts of the *M* parallel channels. The receiver discards the sub-carriers with deep fading and recovers the source data by only collecting the well-received packets from high-energy sub-carriers. With this approach, the quantization of the ADCs can be coarse. Correspondingly, this novel coding scheme can afford a higher noise floor level.

In this paper, we investigate the performance of opportunistic error correction with respect to mitigating noise and interference. It will be verified over the TGn MIMO channel model [19] in C++ simulation. Simulation may show a too optimistic receiver performance. The uncertainties in the real life are mainly simplified assumptions in the simulation like perfectly known noise levels, additive Gaussian noise, omitted synchronization, etc. Therefore, we also will evaluate the performance of the opportunistic error correction scheme in the real-world.

The outline of this paper is as follows. We first discuss the advantages and disadvantages between the joint coding scheme and the separate coding scheme for the MIMO-OFDM channel. Then, opportunistic error correction is depicted in Section III. In Section IV, we describe the system model by showing how we apply this novel coding scheme in MIMO-OFDM systems. After that, we compare its performance with the Forward Error Correction (FEC) layers from the IEEE 802.11n standard [14] over a TGn channel in simulation. Furthermore, we evaluate its performance in practical system. The paper ends with a discussion of the conclusions.

II. Coding Over MIMO-OFDM Channels

MIMO systems increase the capacity of rich scattering wireless channels enormously by using multiple antennas at both the transmitter and the receiver [20-21]. The wireless channel is a hostile environment and often modeled as a frequency selective fading channel. Combining MIMO with OFDM provides an effective solution to frequency selective fading channels. MIMO-OFDM transforms a frequency selective MIMO system into a number of flat fading MIMO systems on different sub-carriers. Still, to achieve reliable communication at a high data rate, error correction codes are required in MIMO-OFDM systems.

In MIMO-OFDM systems, decoding is done after the effect of the MIMO channel is inverted. Correspondingly, coding is performed in the frequency domain of the M parallel channels. Whether source bits are encoded jointly or separately over all the sub-carriers of the channel vector depends on the transmission scheme. There are two schemes to transmit an encoded packet [22]:

- *Scheme I* is to transmit a packet over all the transmitted antennas and over all the sub-carriers like the IEEE 802.11n standard. In such a case, the coding is done jointly over all the sub-carriers of those M parallel channels.
- *Scheme II* transmits a packet over a single sub-carrier per antenna. Using this scheme, the coding is carried out separately over all the sub-carriers of the channel vector.

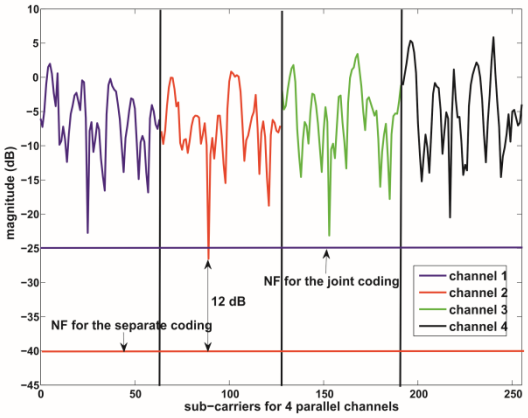

Figure 1. The difference in the required NF between the joint coding.

For a finite block length, coding jointly over all the sub-carriers yields a smaller error probability than can be achieved by coding separately at the same rate [1]. Using the joint coding scheme, sub-carriers with high energy can compensate for those in deep fading. The maximum NF endured by the joint coding is limited to the dynamic range of the M parallel channels, while the maximum NF for the separate coding scheme depends on the sub-carrier with the lowest energy. Let us take an example to show their difference in the required NF. Assume that some encoded packets are transmitted over a 4×4 channel as shown in Fig. 1 and that a packet is received correctly when the $\mathrm{SNR}\geq12$ dB. In this example, the maximum NF for the joint coding is -25 dB. For the separate coding, the maximum NF is determined by the sub-carrier with the lowest energy (i.e. -40 dB in this example). This shows the joint coding scheme performs better than the separate coding scheme at the same NF [1]. Therefore, the current MIMO-OFDM systems utilize the joint coding scheme such as the IEEE 802.11n system [14].

However, the joint coding scheme is not energy-efficient. With this coding method, it is not beforehand known whether the received packet is decodable at a high probability or not at all, which may lead to a waste of processing power. This does not happen in the separate coding scheme, since each sub-carrier can be modeled as a flat fading channel. With the separate coding scheme, the receiver is able to process the well-received packets. Also, because each sub-carrier is considered to be equally important, the NF at the joint coding scheme is limited to the dynamic range of the channel (D). Higher D means lower NF. Correspondingly, higher resolution ADCs need to be used. If we are allowed to discard sub-carriers with deep fading, the NF can be further increased. In such a case, the received signal can be quantized coarsely. To

achieve this, we propose a novel cross coding scheme based on fountain codes which will be explained in the next section.

III. Opportunistic Error Correctioin

Opportunistic error correction is based on fountain codes. A fountain code has a similar property as a fountain of water: when you fill a cup from the fountain, you do not care about what drops of water fall in, but you only want that your cup fills enough to quench your thirst [23]. In other words, fountain-encoded packets are independent with respect to each other. Fountain codes are designed for erasure channels. To apply fountain codes in wireless channels, good error correction codes should be used to make noisy wireless channels behave like an erasure channel. The key point of opportunistic error correction is to trade the code rate of error correction codes with the sub-carriers in deep fading over M parallel channels. By using an error correcting code with a relatively high code rate to encode one fountain-encoded packet and transmitting it over a single sub-carrier per antenna, some parts of the channel vector with deep fading can be discarded. That corresponds to a reduction in the dynamic range of the channel vector. Consequently, lower resolution ADCs can be used in comparison to the joint coding scheme. Besides, using Scheme II to transmit fountain-encoded packets gives the advantage of the separate coding scheme (i.e. saving the processing power).

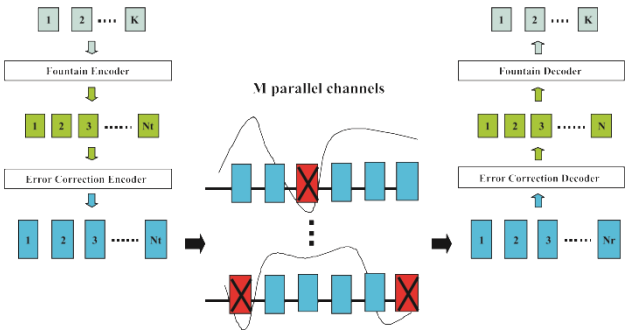

Figure 2. Opportunistic error correction for a $M \times M$ MIMO-OFDM system.

Fig. 2 shows how opportunistic error correction works in MIMO-OFDM systems. With a fountain code, the transmitter can generate a potentially infinite supply of fountain-encoded packets. In this paper, the transmitter generates N_t fountain-encoded packets. Each packet is encoded by an error correction code to convert the wireless channels into erasure channels. After that, each packet is transmitted over a single sub-carrier per antenna. Multiple packets are transmitted simultaneously, using frequency division multiplexing and space division multiplexing. For MIMO-OFDM systems, decoding is always done after inverting the effect of the MIMO channel. Equivalently, fountain-encoded packets are transmitted over a single sub-carrier of the channel vector.

At the receiver, the channel vector is first estimated. With the channel knowledge, the receiver makes a decision about which packet can go through the whole receiving chain. We assume that N_r ($N_r \le N_t$) fountain-encoded packets can go through the error correction decoding. Packets only survive if they succeed in the error correction decoder. The number of fountain-encoded packets N ($K < N \le N_r$) required at the fountain decoder is slightly larger than the number of source packets K :

$$N = (1+\varepsilon)K \tag{1}$$

where ε is the percentage of extra packets and called the overhead.

The mathematical principle behind the fountain decoding is to solve K unknown parameters from N linear equations. It can be solved by Gaussian elimination at high complexity. Therefore, the message-passing algorithm [24] is usually chosen to decode fountain codes. The message-passing algorithm has a linear computation cost [25], but it requires a larger ε for small block size. For example, the practical overhead of LT codes is 14% when $K = 2000$, which limits its application in the practical system [26]. By combining message-passing algorithm with Gaussian elimination, the overhead of LT codes is reduced to 3% when $K \ge 500$ [26].

In this paper, we use *Luby-Transform* (LT) codes [27] as fountain codes and the (175,255) LDPC code [28] with a 7-bit *Cyclic Redundancy Check* (CRC) [29] as error correction codes in the proposed scheme. This new scheme is generic. Any fountain codes can be used (e.g. Raptor codes [30] and online codes [31]). Also, any error correction code (e.g. Turbo codes [32]) can be applied in it. To have a small ε for small K, we choose to decode LT codes by combing the message passing algorithm and Gaussian elimination in this paper.

IV. System Model

The opportunistic error correction scheme is based on fountain codes which have been explained in the above section. This novel method can be applied in the MIMO-OFDM system. In this paper, we take the IEEE 802.11n system as an example of MIMO-OFDM systems.

The current IEEE 802.11n standard gives two options for the FEC layer. One is based on *Rate Compatible Punctured Codes* (RCPC) and the other one is based on LDPC codes [33-35]. RCPC has good performance for random bit errors but performs less for burst bit errors. Interleaving is applied before the RCPC encoding to reduce burst bit errors. Each encoded packet is transmitted based on Scheme I. Although this solution works well in practice, it is not optimal from the power consumption point of view:

- The maximum level of NF (i.e. the lowest resolution of ADCs) is limited to the dynamic range of the parallel channel vector.

- Packets encountered by a "bad" channel are still processed by the receiver.

Those problems can be solved by using opportunistic error correction, as shown in Fig. 3. The key idea is to generate additional packets by the fountain encoder and transmit each packet over a single sub-carrier per antenna. In such a case, the dynamic range of the parallel channel vector can be reduced by discarding the sub- carriers with deep fading. Besides, the receiver does not have to process all the packets but only the well-received packets.

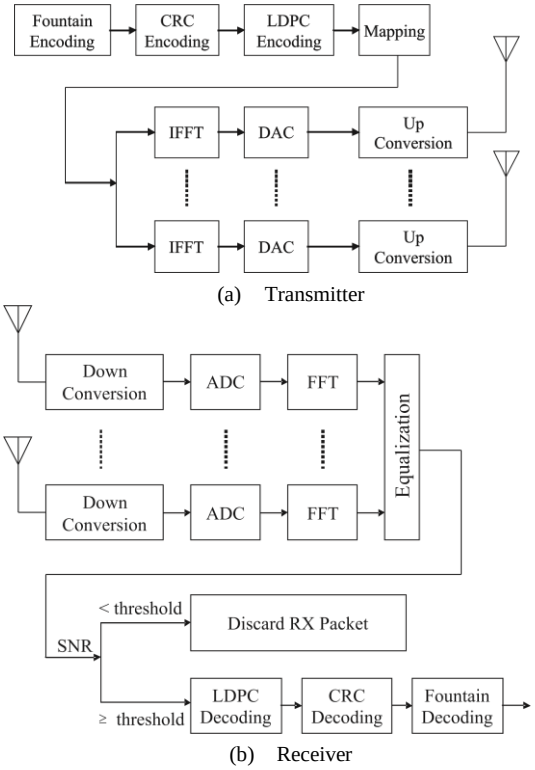

Figure 3. The application of opportunistic error correction in the IEEE 802.11n system: the transmitter (top) and the receiver (bottom).

At the transmitter, the source file is first divided into a set of source packets which are encoded by a LT code. Then, each fountain-encoded packet is added by a 7-bit CRC checksum and encoded by the (175,255) LDPC code. Afterwards, they are mapped into complex symbols before the OFDM modulation.

The $M \times M$ channel output at the n_{th} moment $\mathbf{r}_n = [r_n^{(1)}, ..., r_n^{(m)}, ..., r_n^{(M)}]$ can be written as:

$$\mathbf{r}_n = \sum_{l=0}^{L-1} \mathbf{h}_l \mathbf{x}_{n-l} + \mathbf{n}_n \tag{2}$$

where $\mathbf{x} = [x^{(1)}, ..., x^{(m)}, ..., x^{(M)}]$ is the transmitted vector, $\mathbf{h}_l$ is the $M \times M$ channel matrix at the l_{th} path and L is the number of channel paths. From [36], we know that $x^{(m)}$ can be modeled as a Gaussian-distributed random variable with zero mean and a variance of 1. The elements in $\mathbf{x}$ are mutual independent, so it has zero mean and a unity covariance matrix. In addition, $\mathbf{x}_n$ and $\mathbf{x}_{n'}$ are mutual independent if $n \neq n'$. $\mathbf{n}_n$ is the channel noise vector (including the quantization noise, the thermal noise and the interference) in the time domain. We assume that the elements in $\mathbf{n}_n$ are mutual independent, so it has zero mean and a covariance matrix of $\sigma^2\mathbf{I}$. Therefore, the *Signal-to-Noise Ratio* (SNR) of the signal at the m_{th} received signal is defined as:

$$\mathrm{SNR}_{r_n^{(m)}} = \frac{M}{\sigma^2} \tag{3}$$

Given the same $\mathrm{SNR}_{r_n^{(m)}}$, the level of NF (i.e. σ^2) increases by 3 dB if *M* doubles.

At the receiver, synchronization and channel estimation can be done using the preambles and the pilots, which are defined in [14]. In this paper, we use the *zero forcing* algorithm [37] to estimate the channel. Each sub-carrier can be considered as a narrow-band MIMO channel:

$$\mathbf{Y}_k^p = \mathbf{H}_k \mathbf{X}_k^p + \mathbf{N}_k^p \tag{4}$$

where $\mathbf{X}_k^p = [X_k^{p(1)}, ..., X_k^{p(M)}]$ is the preamble at the k_{th} sub-carrier and $\mathbf{N}_k^p = [N_k^{p(1)}, ..., N_k^{p(M)}]$ is the noise in the frequency domain:

$$\mathbf{N}_k^p = \frac{1}{\sqrt{N}} \sum\nolimits_n \mathbf{n}_n^p e^{-j\frac{2\pi}{N}nk} \tag{5}$$

where N is the number of sub-carriers. According to the *Central Limit Theorem*, $N_k^{p(m)}$ is Gaussian-distributed with zero mean and a variance of σ^2 [38]. $\mathbf{H}_k$ is the fading matrix at the k_{th} sub-carrier defined by:

$$\mathbf{H}_k = \sum_{l=0}^{L-1} \mathbf{h}_l e^{-j\frac{2\pi}{N}lk} \tag{6}$$

which can be estimated by the zero-forcing algorithm as [1]:

$$\begin{aligned} \mathbf{H}_k &= \mathbf{Y}_k^p \mathbf{X}_k^{p+} \\ &= \mathbf{H}_k + \mathbf{N}_k^p \mathbf{X}_k^{p+} \end{aligned} \tag{7}$$

where $\mathbf{X}_k^{p+}$ is the pseudoinverse of the matrix $\mathbf{X}_k^p$.

In order to detect the transmitted symbol from each transmitted antenna, equalization needs to be done. In this paper, the zero-forcing algorithm is used to invert the effect of the MIMO channel:

$$\begin{aligned} \mathbf{X}_k &= \mathbf{H}_k^+ \mathbf{Y}_k \\ &= \left(\mathbf{H}_k + \mathbf{N}_k^p \mathbf{X}_k^{p+}\right)^+ \left(\mathbf{H}_k \mathbf{X}_k + \mathbf{N}_k\right) \end{aligned} \tag{8}$$

With the perfect channel estimation, the above equation can be simplified as:

$$\mathbf{X}_k = \mathbf{X}_k + \mathbf{H}_k^+ \mathbf{N}_k \tag{9}$$

Thus, for the symbol $X_k^{(m)}$ from the m_{th} antenna at the k_{th} sub-carrier, its SNR can be derived as:

$$\mathrm{SNR}_k^{(m)} = \left(\sigma^2 \sum_{s=0}^{M-1} \left| \mathbf{H}_k^{+(m,s)} \right|^2 \right)^{-1} \quad (10)$$

In such a case, the receiver can decide which packets should go through the receiving chain. Only if its SNR is equal to or above the threshold, the received packet will go through the LDPC decoder otherwise it will be discarded. Correspondingly, the processing power can be reduced.

However, the channel estimation and the equalization are based on the zero-forcing algorithm whose accuracy and complexity are low. In such a case, the receiver can hardly predict correctly whether the received packet is decodable at a high probability, as we can see in Eq. (8) by the presence of the term $\mathbf{N}_k^p \mathbf{X}_k^{p+}$. That degrades its performance. To avoid it, the receiver will process all the fountain-encoded packets with non-perfect channel estimation. The received packets can only survive if they pass the LDPC decoder and the CRC decoder successfully. When the receiver collects enough fountain-encoded packets, it starts to recover the source data by using the message-passing algorithm and Gaussian elimination algorithm.

V. Performance Analysis In Simulations

In this section, we analyze the performance of opportunistic error correction in MIMO-OFDM systems by comparing the following FEC schemes:

- FEC I: RCPC with interleaving from the IEEE 802.11n standard.
- FEC II: LDPC codes from the IEEE 802.11n standard with n = 648.
- FEC III: opportunistic error correction.

The IEEE 802.11n system is taken as an example of MIMO-OFDM systems. 52 sub-carriers are used to transmit data as defined in [14]. To have the same code rate (i.e. R = 0.5), FEC III is allowed to discard around 21% in the simulation. $21\% \approx 1 - \frac{R}{R_1 \cdot R_2}$, where R is the effective code rate (i.e. 0.5), R_1 is the code rate of LT codes (i.e. $\frac{1}{1.03} \approx 0.97$) and R_2 is the code rate of the (175,255) LDPC code with 7-bit CRC (i.e. $\frac{168}{255} \approx 0.66$).

For each simulation point, we transmit more than 1000 bursts of data (i.e. more than 100 million bits) over a 20 MHz downlink TGn channel. Each burst consists of 630 source packets with a length of 168 bits. The source file is encoded by FEC I, II and III, respectively. With FEC III, each burst is encoded by a LT code (with parameter $c = 0.03, \delta = 0.3$) and decoded by the message-passing algorithm and Gaussian elimination together. Only 3% overhead is required to reconstruct the original data successfully [26]. To each fountain-encoded packet, a 7-bit CRC is added before the (175,255) LDPC encoding is applied. Before the OFDM modulation, the encoded bits are mapped into QAM-16 symbols.

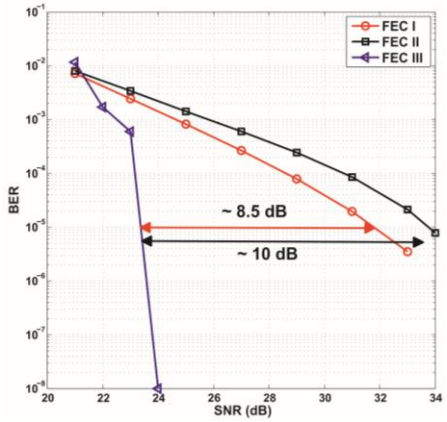

(a) 2-by-2 with perfect H

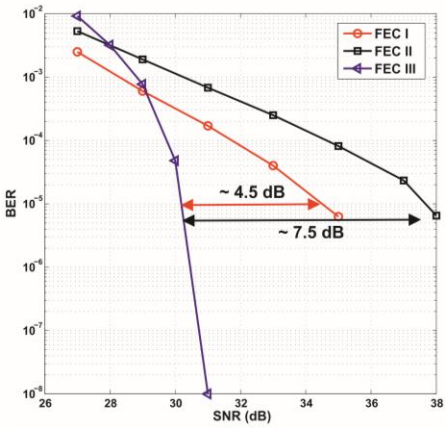

(b) 4-by-4 with perfect H

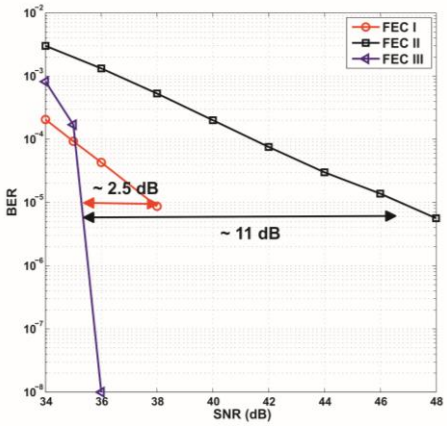

(c) 8-by-8 with perfect H

Figure 4. Performance comparison between FEC I, II and III at R=0.5 over the TGn channel at 20 MHz. We compare them in three systems: the 2×2 system, the 4×4 system and the 8×8 system. FEC III can achieve error-free when the fountain decoder received enough fountain-encoded packets. We represent BER = 0 by 10^{-8} in the above figures.

In total, we compare them in three types of MIMO-OFDM systems: the 2×2 system, the 4×4 system and the 8×8 system. Fig. 4 shows the simulation results with perfect synchronization and channel estimation. From this figure, we can see the follows.

- In the case of FEC I, it has a BER of 10^{-5} or lower when $\mathrm{SNR} \geq 31.5$ dB in the 2×2 system,

$SNR \geq 34.5$ dB in the 4×4 system and $SNR \geq 38$ dB in the 8×8 system. FEC I has a SNR loss of around 3 dB when M doubles. Given the same level of noise floor, Eq. (3) shows that SNR increases by 3 dB if *M* doubles. Hence, the maximum NF endured by FEC I is not affected if the multiplexing gain doubles.

- In the case of FEC II, it reaches a BER of 10^{-5} or lower when $SNR \geq 34$ dB in the 2×2 system, $SNR \geq 37.5$ dB in the 4×4 system and $SNR \geq 46.5$ dB in the 8×8 system. When *M* increases from 2 to 4, FEC II could survive at the same NF to achieve a BER of 10^{-5} or lower (i.e. a SNR gain loss of around 3.5 dB). However, the maximum NF in the 8×8 system has to be 6 dB lower than in the 4×4 system for FEC II to have a BER of 10^{-5} or lower.
- In the case of FEC III, it can achieve error free when $SNR \geq 24$ dB in the 2×2 system, $SNR \geq 31$ dB in the 4×4 system and $SNR \geq 36$ dB in the 8×8 system. FEC III loses more than 3 dB when *M* doubles. To have the error-free quality, the maximum NF for FEC III has to be decreased as *M* increases. When *M* changes from 2 to 4, NF has to be decreased by 4 dB. When *M* doubles from 4 to 8, NF has to be decreased by 2 dB.
- With respect to FEC I, FEC III has a SNR gain of around 8.5 dB in the 2×2 system, around 4.5 dB in the 4×4 system and around 2.5 dB in the 8×8 system. The SNR gain decreases with *M*.
- In comparison with FEC II, FEC III has a SNR gain of around 10 dB in the 2×2 system, around 7.5 dB in the 4×4 system and around 11 dB in the 8×8 system. The SNR gain decreases when *M* increases from 2 to 4 and increases as *M* changes from 4 to 8.

The maximum NF endured by FEC I is not affected by *M*; while the maximum NF for FEC III has to be decreased as *M* increases. Still, FEC III requires lower SNR than FEC I and II to achieve $BER \leq 10^{-5}$dB in three MIMO-OFDM systems. Therefore, we can conclude that opportunistic error correction (i.e. FEC III) works best with respect to the joint coding schemes (i.e. FEC I and II) in the IEEE 802.11n standard.

VI. Practical Evaluation

The C++ simulation results in the above section show the performance of opportunistic error correction in comparison with the joint coding scheme (i.e. FEC I and II) for three types of MIMO-OFDM systems. However, simulation may show a too optimistic receiver performance. In this section, we evaluate its performance in practice and investigate whether opportunistic error correction is more robust to the real-world's imperfections.

A. System Setup

The practical experiments are done in the experimental communication testbed designed and realized by Signals and Systems Group [39], University of Twente, as shown in Fig. 5. It is a 2×2 MIMO system, which is assembled as a cascade of the following modules: PC, DACs, RF up-converters, power amplifiers, antennas, and the reverse chain for the receiver. At the receiver, there are no power amplifiers and band-pass RF filters before the down-converters but two low-pass baseband filters before the ADCs to remove the aliasing.

1) The transmitter: The data is generated offline in C++. The generation consists of the random source bits selection, the FEC encoding and the digital modulation as we depict in Section IV. The generated data is stored in a file. A server software in the transmit PC uploads the file to the Adlink PCI-7300A board (80 MB/s High-Speed 32-CH Digital I/O PCI Card) which transmits the data to DAC (AD9761, 10-Bit, 40 MSPS, dual Transmit D/A Converter) via the FPGA board. After the DAC, the baseband analog signal is up-converted to 2.3 GHz by a Quadrature Modulator (AD8346, 2.5 GHz Direct Conversion Quadrature Modulator) and transmitted using two conical skirt monopole antennas.

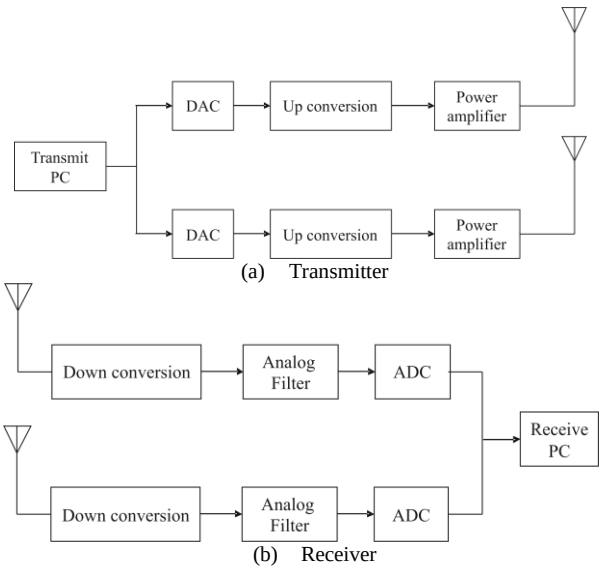

Figure 5. Block diagram of the 2×2 MIMO testbed.

2) The Receiver: The reverse process takes place at the receiver. The received RF signal is first down-converted by a Quadrature Demodulator (AD8347, 2.5 GHz Direct Conversion Quadrature Demodulator), then passes the 8th order low-pass Butterworth analog filter to remove the aliasing. The baseband analog signal is quantized by the ADC (AD9238, Dual 12-Bit, 20/40/65 MSPS, 3V A/D Converter) and stored in the receive PC via the Adlink PCI board.

The received data is processed offline in C++. The receiver should synchronize with the transmitter and estimate the channel using the preambles and the pilots, which are defined in [14]. Timing and frequency synchronization is done by the Schmidl & Cox algorithm [40] and the channel is estimated by the *zero forcing* algorithm. In addition, the *residual carrier frequency*

offset is estimated by the four pilots in each OFDM symbol [41]. Before the decoding starts, the effect of the MIMO channel has to be inverted with the estimated channel knowledge. As shown in Eq. (8), the real SNR of $\mathbf{X}_k$ can not be estimated reliably. That degrades the performance of opportunistic error correction if we only process the packets with a high estimated SNR. Hence, we process all the received fountain-encoded packets in practice.

B. Experiment Setup

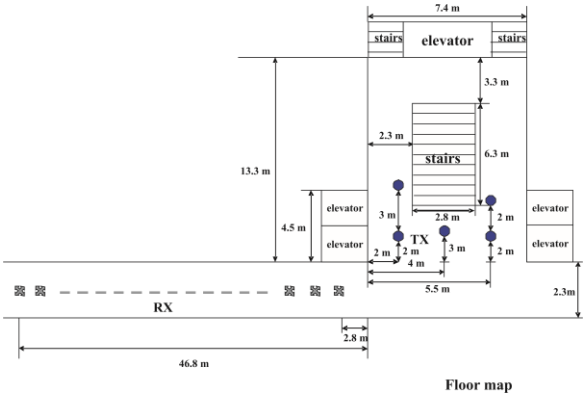

Figure 6. Experiment setup: antennas are 0.9 m above the concrete floor. The experiments are done in the corridor of the Signals and Systems Group. The receiver is positioned at the left side of the corridor (i.e. the cross positions) and the transmitter is at the circle positions as shown in the figure. The hall contains one coffee machine, one garbage bin and one glass cabin.

In Section V, these FEC schemes have been compared in the C++ simulation. In the simulation, they can be compared by using the same source bits. Different channel bits can go through the same random frequency selective channels. However, it does not apply in the real environment. The wireless channel is time-variant even when the transmitter and the receiver are stationary (e.g. the moving of the elevator with the closed door can affect the channel). Hence, we should compare them by using the same channel bits.

Because not every stream of random bits is a codeword of a certain coding scheme, it is not possible to derive its corresponding source bits from any sequence of random bits, especially for the case of FEC I and FEC III. Fortunately, the decoding of FEC II is based on the parity check matrix. Any stream of random bits can have its unique sequence of source bits with its corresponding syndrome matrix. The receiver can decode the received data based both on the parity check matrix and the syndrome matrix. Thus, FEC I can use the same channel bits with FEC II, same for FEC II and FEC III. In such a case, they can be compared under the same channel condition (i.e. channel fading, channel noise and the distortion caused by the hardware.). During the experiments, both sequences of channel bits are transmitted in one burst (i.e. 2 blocks) in order to have their channels as similar as possible.

In the experiments, we transmit more than 2500 blocks of source packets over the air. Each block consists of 105840 source bits. The source bits are encoded by FEC I and III, respectively. The encoded bits are shared with FEC II as just explained. Afterwards, they are mapped into QPSK symbols before the OFDM modulation.

Each experiment corresponds to the fixed position of the transmitter and the receiver. It is possible that some experiments might fail in decoding. Due to the lack of the feedback channel in the testbed, no retransmission can occur. In this paper, we assume that the experiment fails if the received data per measurement has a BER higher than 10^{-3} by using FEC I and II. For the case of FEC III, if the packet loss is more than 21% as expected, we assume that the experiment fails.

C. Experiment Results

In total, 180 experiments have been done. There are 14 blocks of data transmitted over each experiment: 7 blocks for FEC I and II and 7 blocks for FEC II and III. As mentioned earlier, the wireless channel is time-variant even when the transmitter and receiver are placed at the same position. So, we are going to analyze the experiments for FEC I and II and those for FEC II and III separately.

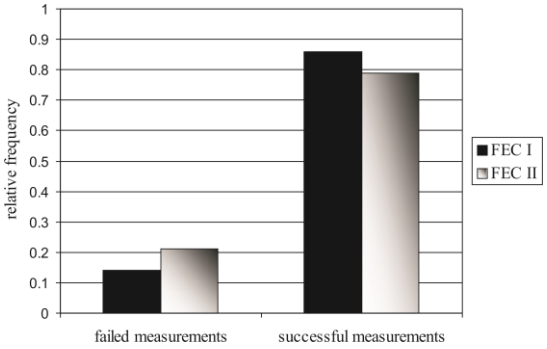

Figure 7. Histogram of the experiment results for FEC I and II. By using FEC I, around 14% of experiments are failed. For the case of FEC II, around 21% of experiments are failed.

1) *FEC I vs. FEC II:* Not every experiment succeeds in decoding. FEC I fails in 14% of experiments while FEC II fails in 21% of experiments, as we can see in Fig. 7. This *concludes* that FEC I works in more channel conditions than FEC II.

Both FEC schemes succeed in 142 experiments, where the SNR of the signal at two receive antennas ranges from 17 dB to 25 dB. In order to investigate whether FEC I can endure higher NF than FEC II as shown in the simulation results, we add extra white noise to the received signal in the software. It is difficult to have the same SNR range in all measurements, so we evaluate the practical performance by analyzing the statistical characteristics of experiment results. Here, we define $\mathrm{SNR}_{\mathrm{I}}$ as the minimum SNR for FEC I and $\mathrm{SNR}_{\mathrm{II}}$ as the minimum SNR for FEC II to reach a BER of 10^{-3} or lower. The difference between $\mathrm{SNR}_{\mathrm{II}}$ and $\mathrm{SNR}_{\mathrm{I}}$ is expressed as:

$$\Delta_{\mathrm{I}} = \mathrm{SNR}_{\mathrm{II}} - \mathrm{SNR}_{\mathrm{I}} \quad (11)$$

If $\Delta_1 > 0$ (i.e. $SNR_{II} > SNR_I$), FEC II needs higher SNR (i.e. lower level of NF) to achieve BER < 10^{-3} than FEC I. $\Delta_1 < 0$ is for the opposite case.

Fig. 8 shows the statistical characteristics of SNR_I, SNR_{II} and Δ_1. Both SNR_I and SNR_{II} have a wide range: $SNR_I \in [10, 24]$ dB and $SNR_{II} \in [9, 25]$ dB. This presents that different channel condition requires different NF to achieve BER < 10^{-3}. In the simulation, all the channel conditions have the same level of NF. Given the same NF (i.e. SNR) in those 142 experiments, SNR_I should be 24 dB and SNR_{II} needs to be 25 dB to have all those experiments with BER < 10^{-3}. In this case, FEC I has a SNR gain of 1 dB over FEC II. Furthermore, Fig. 8(b) shows whether FEC I performs better than FEC II in every experiment. Δ_1 ranges from -2 dB to 5 dB. Around 86% of experiments have Δ_1 within 1 dB. The average Δ_1 is around 0.06 dB. That leads to the following conclusion. In comparison with FEC II, FEC I has a SNR gain of 1 dB with the same NF in all experiments (i.e. 142 experiments) and an average SNR gain of around 0.06 dB when every experiment has its own maximum NF.

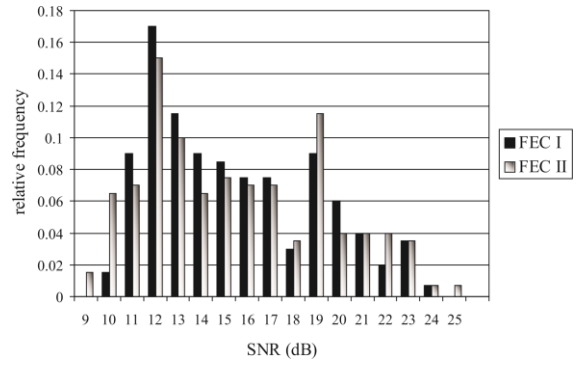

(a) Histogram of SNR_I and SNR_{II}

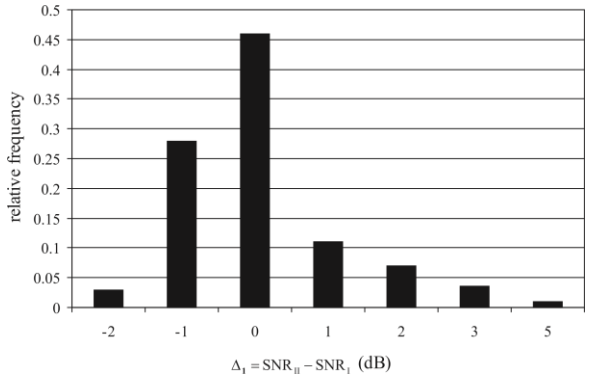

(b) Histogram of Δ_1

Figure 8. Histogram of SNR_I, SNR_{II} and Δ_1.

2) FEC II vs. FEC III: Fig. 9 is the statistical analysis of the *experiment* data shared by both FEC II and III. From this figure, we can see that FEC II fails in 19% of experiments and FEC III fails only in 8% of experiments. Fig. 7 and Fig. 9 present that opportunistic error correction (i.e. FEC III) survives in more channel conditions than the joint coding scheme (i.e. FEC I and II).

FEC II and III succeed in 145 experiments. In those experiments, the SNR of the signal at two receive antennas ranges from 17 dB to 25 dB. Same as the above section, we add extra white noise to the received signal in the software. We define SNR_{III} as the minimum SNR for FEC III to reach the error-free quality. The difference between SNR_{II} and SNR_{III} is expressed as:

$$\Delta_2 = SNR_{II} - SNR_{III} \quad (12)$$

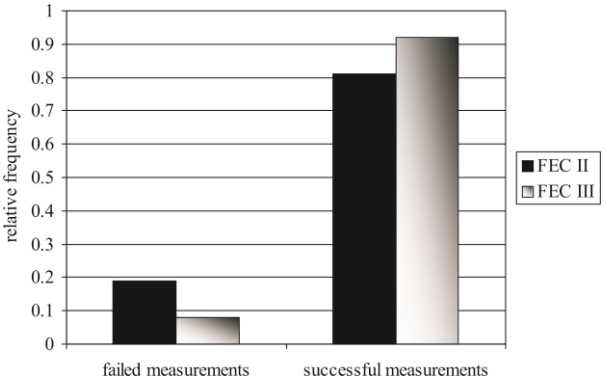

Figure 9. Histogram of the experiment data for FEC II and III. By using FEC II, around 19% of experiments are failed. For the case of FEC III, around 8% of experiments are failed.

If $\Delta_2 > 0$ (i.e. $SNR_{II} > SNR_{III}$), FEC II needs higher SNR (i.e. lower level of NF) to achieve BER<10^{-3} than FEC III to have the error-free quality. $\Delta_2 < 0$ is for the opposite case.

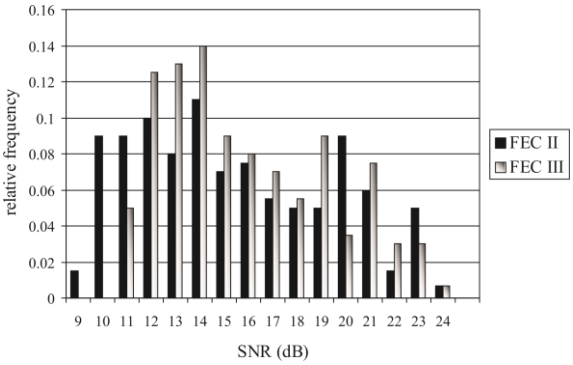

(a) Histogram of SNR_{II} and SNR_{III}

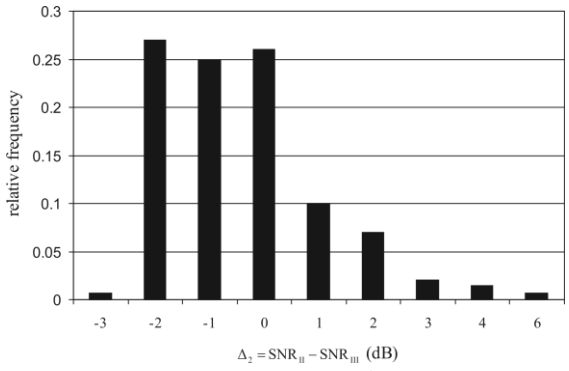

(b) Histogram of Δ_2

Figure 10. Histogram of SNR_{II}, SNR_{III} and Δ_2.

Fig. 10 shows the statistical characteristics of SNR_{II}, SNR_{III} and Δ_2. SNR_{II} and SNR_{III} have a wide range: $SNR_{II} \in [9,24]$ dB and $SNR_{III} \in [11,24]$ dB. The maximum values of SNR_{II} and SNR_{III} are the same (i.e. 24 dB). Hence, with the same NF in those 145 experiments, FEC III has no SNR gain comparing to FEC II. However, the minimum SNR_{II} is 9 dB but the minimum SNR_{III} is 11 dB. That means that FEC II requires less SNR to achieve BER$<10^{-3}$ than FEC III to reach error free in some experiments. Fig. 10(b) presents whether FEC II performs better than FEC III in every experiment. Δ_2 ranges from -3 dB to 6 dB. Around 78% of experiments have Δ_2 in the range of [-2,0] dB, which means that FEC II does not require higher SNR than FEC III to reach the required BER. On average, Δ_2 is around -0.4 dB. Therefore, we can conclude that FEC III can survive in more channel conditions than FEC II, but the average SNR required by FEC III is larger than FEC II in the successful experiments.

VII. Conclusions

Opportunistic error correction based on fountain codes is designed for MIMO-OFDM systems to reduce the power consumption in ADCs. Fountain codes are designed for erasure channels. To apply fountain codes to the wireless channel, error correcting codes have to be used in every fountain-encoded packet. The key idea of this scheme is the tradeoff between the code rate of error correcting codes and the sub-carriers in deep fading. By transmitting a fountain-encoded packet over a single sub-carrier per antenna, fountain codes can reconstruct the original file by only using the packets transmitted over the sub-carriers with high-energy. In this way, the ADC does not have to take care of each part of those *M* parallel channels. The received signal can be quantized coarsely. The coarse quantization means a higher level of noise floor.

In this paper, we have investigated its performance over the TGn channel in the aspect of mitigating the noise and the interference. In the simulation, we compare three FEC layers in different MIMO-OFDM systems with the same coding rate (i.e. *R*=0.5) and the modulation scheme (i.e. QAM-16): RCPC with interleaving from the IEEE 802.11n standard (i.e. FEC I), the (324,648) LDPC code from the IEEE 802.11n standard (i.e. FEC II) and opportunistic error correction based on fountain codes (i.e. FEC III). FEC III works better than FEC I and II in the simulation. With respect to FEC I, FEC III has a SNR gain of around 8.5 dB in the 2×2 system, around 4.5 dB in the 4×4 system and around 2.5 dB in the 8×8 system. Their SNR difference decreases with *M*. However, in comparison with FEC II, FEC III has a SNR gain of around 10 dB in the 2×2 system, around 7.5 dB in the 4×4 system and around 11 dB in the 8×8 system. The SNR gain decreases when *M* increases from 2 to 4 then increases as M changes from 4 to 8.

Furthermore, we have evaluated their performance in practice. The real wireless channel is time-variant, so FEC I and II share the same channel bits to have the same channel condition. Same for FEC II and III. FEC III survives in the most experiments (i.e. 92%) which is followed by FEC I (i.e. 86%) and FEC II (i.e. around 80%). Correspondingly, FEC III works in more channel conditions than FEC I and II. With the same level of NF, FEC II requires the same level of noise level as FEC III to let all 145 experiments reach the required BER (i.e. BER$<10^{-3}$ for FEC II and BER=0 for FEC III). However, FEC III has an average SNR loss of around 0.4 dB if the level of NF in every experiment is adjusted to the maximum value.

References

[1] D. Tse and P. Viswanath, *Fundamentals of Wireless Communication*, New York, NY, USA: Cambridge University Press, 2005.

[2] A. Paulraj, R. Nabar, and D. Gore, *Introduction to Space-Time Wireless Communications*, Cambridge University Press, 2003.

[3] T. Kaiser and A. Bourdoux, *Smart Antennas, State of the Art.* Hindawi Pub Corp, 2005.

[4] E. Biglieri, R. Calderbank, and A. Constantinides, *MIMO Wireless Communications.* Cambridge University Press, 2007.

[5] K. Fazel and S. Kaiser, *Multi-carrier and Spread Spectrum Systems*, Wiley, 2003.

[6] M. Gast, *802.11 Wireless Networks: the Definitive Guide.* O'Reilly Media, Inc., 2005.

[7] H. Liu and G. Li, *OFDM-based Broadband Wireless Networks, Design and Optimization.* Wiley-Interscience, 2005.

[8] J. Thomoson, *et al.*, "An integrated 802.11a baseband and MAC processor," in *Proc. IEEE International Solid-State Circuits Conference, Digest of Technical Papers*, vol. 1, 2002, pp. 126-451.

[9] B. Murmann, "A/D converter trends: Power dissipation, scaling and digitally assisted architectures," in *Proc. IEEE Custom Integrated Circuits Conference*, 2008, pp. 105-112.

[10] M. Bossert, *Channel Coding for Telecommunications*, John Wiley & Sons, Inc., New York, USA, 1999.

[11] R. G. Gallager, *Information Theory and Reliable Communication*, John Wiley & Sons, Inc., New York, USA, 1968.

[12] A. Carlson, *Communication Systems*, McGraw-Hill, New York, 1975.

[13] IEEE, *Wireless LAN Medium Access Control (MAC) and Physical Layer (PHY) Specifications, High-Speed Physical Layer in the 5GHz Band*, IEEE 802.11a Standard, Part 11 1999.

[14] IEEE, *Draft Standards for wireless LAN Medium Access Control (MAC) and Physical Layers (PHY) Specifications, Enhancements for Higher Throughput*, IEEE 802.11n Standard, Part 11, Jan 2007.

[15] *Digital Video Broadcasting (DVB); Transmission System for Handheld Terminals (DVB-H)*, European Telecommunications Standards Institute , Nov. 2004.

[16] *Digital Video Broadcasting (DVB); Framing Structure, Channel Coding and Modulation for Digital Terrestrial Television*, European Telecommunications Standards Institute, ETSI EN 300 744, V.1.5.1, 2004.

[17] *Framing Structure, Channel Coding and Modulation for A Second Generation Digital Terrestrial Television Broadcasting System (DVB-T2)*, European Telecommunications Standards Institute, Jun 2008.

[18] V. Erceg, L. Schumacher, P. Kyritsi, *et al.*, "TGn channel models," *IEEE 802.11 Document 802.11-03/940r4*, 2004.

[19] L. Schumacher and B. Dijkstra, "Description of a MATLAB® implementation of the indoor MIMO WLAN channel model proposed by the IEEE 802.11 TGn channel model special committee," in *Implementation Note Version*, 2004.

[20] G. Foschini and M. Gans, "On limits of wireless communications in a fading environment when using multiple antennas," *Wireless Personal Communcations*, vol. 6, no. 3, pp. 311-335, 1998.
[21] I. Telatar, "Capacity of multi-antenna gaussian channels," *European Transactions on Telecommunications*, 1999.
[22] R. Prasad, M. Rahman, and S. Das, *Single-band Multi-Carrier MIMO Transmission for Broadband Wireless Systems.* River Publisher, 2009.
[23] M. Mitzenmacher, "Digital fountains: A survey and look forward," in *IEEE Information Theory Workshop*, 2004, pp. 271-276.
[24] D. MacKay, *Information Theory, Inference and Learning Algorithms*, Cambridge University Press, UK, 2003.
[25] D. Mackay, "Fountain codes," *IEEE Communications*, vol. 152, no. 6, pp. 1062-1068, 2005.
[26] X. Shao, R. Schiphorst, and C. H. Slump, "An opportunistic error correction layer for OFDM systems," *EURASIP Journal on Wireless Communications and Networking*, 2009.
[27] M. Luby, "LT codes," in *Proc. 43rd Annual IEEE Symposium on Foundations of Computer Science*, 2002, pp. 271-282.
[28] Y. Kou, S. Lin, and M. Fossorier, "Low-density parity-check codes based on finite geometries: A rediscovery and new results," *IEEE Transactions on Information Theory*, vol. 47, no. 7, pp. 2711-2736, 2001.
[29] W. Peterson and D. Brown, "Cyclic codes for error detection," *Proceedings of the IRE*, vol. 49, no. 1, pp. 228-235, 1961.
[30] A. Shokrollahi, "Raptor codes," *IEEE Transactions on Information Theory*, vol. 52, 2006.
[31] P. Maymounkov, "Online codes," *Research Report TR 2002-833*, New York University, 2002.
[32] C. Berrou, A. Glavieux, and P. Thitimajshima, "Near Shannon limit error-correcting coding and decoding: Turbo codes," in *IEEE International Conference on Communications*, 1993.
[33] R. G. Gallager, *Low-Density Parity-Check Codes*, MIT Press, 1963.
[34] D. MacKay and R. Neal, "Good codes based on very sparse matriices," *Cryptography and Coding*, pp. 100-111, 1995.
[35] T. Richardson, M. Shokrollahi, and R. Urbanke, "Design of capacity-approaching irregular low-density parity-check codes," *IEEE Transactions on Information Theory*, vol. 47, no. 2, pp. 619-637, 2001.
[36] X. Shao and C.H. Slump, "Quantization effect in OFDM systems," in *Proc. 29th Symposium on Information Theory in the Benelux*, Leuven, May 2008.
[37] T. Rappaport, *Wireless Communications: Principles and Practice*, Prentice Hall, New Jersey, 2002.
[38] X. Shao and C. H. Slump, "Opportunistic error correction for MIMO," in *20th Personal, Indoor and Mobile Radio Communications Symposium*, Tokyo, Japan, 2009.
[39] H. S. Cronie, F. W. Hoeksema, and C. H. Slump, "A CSP-based processing architecture for a flexible MIMO-OFDM testbed," in *Proc. Communications Process Architectures Symposium*, Enschede, The Netherlands, 2003.
[40] T. Schmidl and D. Cox, "Robust frequency and timing synchronization for OFDM," *IEEE Transactions on Communications*, vol. 45, no. 12, pp. 1613-1621, 1997.
[41] K. Akita, R. Sakata, and K. Sato, "A phase compensation scheme using feedback control for IEEE 802.11a receiver," in *IEEE 60th Vehicular Technology Conference*, vol. 7, 2004.

Dr. Xiaoying Shao received her M.Sc degree in Electrical Engineering from University of Twente, The Netherlands in 2006. In 2010, she obtained her Ph.D degree in Wireless Communications from University of Twente, The Netherlands. Currently, she is the postdoc at the same group and working in the `The 2D Coding' project. Meanwhile, she is active in biometric template protection. Her research interest mainly lies in signal processing and information theory for communication systems, data storage and biometric recognition systems.

Dr. Cornelis H. Slump received the M.Sc. degree in Electrical Engineering from Delft University of Technology, Delft, The Netherlands in 1979. In 1984 he obtained his Ph.D. in physics from the University of Groningen, The Netherlands. From 1983 to 1989 he was employed at Philips Medical Systems in Best as head of a predevelopment group on medical image processing. In 1989 he joined the Network Theory group from the University of Twente, Enschede, The Netherlands. His main research interest is in digital signal processing, including realization of algorithms in VLSI.